Uncertain solutions and multiple steady states in the built ventilation flows

Hang Xu[1], *Hong-Liang* Zhang[1], *Wei-Wei* Wang[1] and *Fu-Yun* Zhao[1*]

[1]Wuhan University, School of Power and Mechanical Engineering, 430072 Wuhan, China

Abstract. In past decades, several peers and not too many publications have reported that uncertain solutions existed in the building ventilation flows. In the present work, numerical, theoretical and experimental researches have been jointly applied for the non-unique flow solutions occurring in the built environment, covering from thermal driven flows, pressure driven flows and multi component flows. General multiple steady flows could be observed when different initial conditions were imposed. Independent flow branch could switch from each other during the critical point or some sudden transitions were imposed. Theoretical solutions could give rough routes for multiple flows, whereas numerical ones could give such detailed transitions delicately. Experimental model results well demonstrated those theoretical and numerical results. Future low carbon ventilation engineering applications could benefit from present fundamental researches.

1 Introduction

Air flow, heat and mass transfer processes are widely involved in practical projects, such as building ventilation, indoor gaseous pollutant transmission, envelope heat and moisture transfer. Non-unique or multiple flow states have been identified within the past decade in the field of built environments [1,2,3,4]. Figure 1 illustrates the different evolution processes of air convection in a single room building. Due to the force

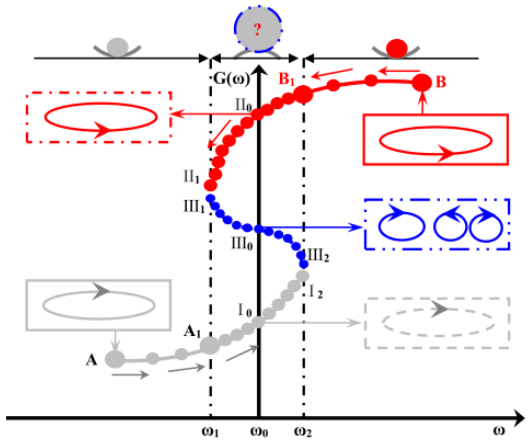

Fig.1. Schematic diagram of multiply solution of indoor air convection in buildings

of external ventilation, internal heat and mass buoyancy or multiple groups of combined, there may be three groups of different flow characteristics [5]. The multiple steady behavior of indoor air convection process from three convection modes are analysed in present work, which can effectively help people take corresponding measures to form an air environment conducive to personnel, make the clean air flow enter the work area, and even achieve the purpose that conventional air flow control methods hardly achieve, For example, greater air change rates and heat dissipation performance are acquired in the working area but less system energy consumption, and cooperate to improve heat diffusion, reduce wet diffusion and so on.

2 Nature convention

It is well known that until a certain critical temperature or concentration difference is exceeded, heat or composition is transferred vertically from bottom to top only by diffusion. But after the critical temperature or concentration difference is surpassed, convection begins, with a significant increase in the overall heat and mass transfer. The confrontation behavior of the latter case may lead to the phenomenon of multiple steady solutions according to the change of boundary conditions.

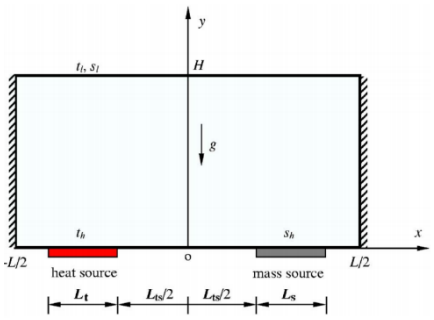

Fig. 2. Nature convention in an enclosure with double diffusive

* Corresponding author: fyzhao@whu.edu.cn

2.1 Physical configuration and model

Geometry and boundary conditions for the studied enclosure with discrete heat and contaminant sources shown in Figure 2. All the physical properties are supposed to be independent of the temperature and concentration, except the mixture density variations, for which the Boussinesq approximation is used. Buoyancy ratio, thermal Rayleigh number, and pitches of heat and pollutant sources all will affect the multiple steady convective solutions. Thermal Rayleigh number will be focused on this section.

2.2 Results and discussion

Apart from the rest state natural solutions, other steady flow states can be obtained if different initial conditions were chosen. Fig. 3(c), the rest state was used as initial conditions, the soulutally driven unicellular core flow spans now completely the enclosure. For this situation, the cold fluid moves down toward the heated element and the less-polluted mixture ascends above the solute element. Heat lines and mass lines both exhibit a counter clockwise heat and mass transfer flow pattern. The thermal and solutal buoyancy forces both accelerate the single-eddy flow and enhance the flow intensity, thus increasing the overall heat transfer rate. However, the overall mass transfer rate is unexpectedly decreased when compared to the second solution of Fig. 3(b).

Fig. 3(a) (b) obtained through gradually decreasing Ra_t from 10^3 to 2×10^4 and 10^6 to 2×10^4, respectively. The results indicate that the flow intensity of Fig. 3(b) remains strong and it is about 25 times higher than that of Fig. 3(a). Upon increasing Ra_t from 10^3, it was found that this flow regime with the symmetric and multicellular weak flow structure depicted in Fig. 3(a), could be maintained up to approximately 2.6×10^4. Beyond 2.6×10^4, an oscillatory state would emerge. This has been deliberately avoided in the present work.

On the contrary, upon decreasing Ra_t from 10^6, the flow regime of high intensity can be maintained until Ra_t is lower than 5.0×10^3. Furthermore, for the third solution, obtained by using the flow configuration of Fig.3(c) as initial conditions, the unicellular flow pattern can be maintained in the range $1.1 \times 10^4 \leq Ra_t \leq 10^6$, where the Nusselt and Sherwood numbers are enhanced and inhibited, respectively, compared with the solution obtained using $Ra_t = 10^6$ as initial conditions.

3 Force convention

In this chapter we analyzed the basic heat transfer question by looking only at forced-convection situations, in which the fluid flow is caused (forced) by an external agent unrelated to the heating effect. The numerical investigations of the multiple flow states in a three-dimensional ventilated room is dedicated. In others research, the bifurcations of three-dimensional fluid flow in slot-ventilated enclosures have not been considered. Three-dimensionality is more realistic in building ventilation, especially when the ventilation forces are opposing and are of comparable magnitude.

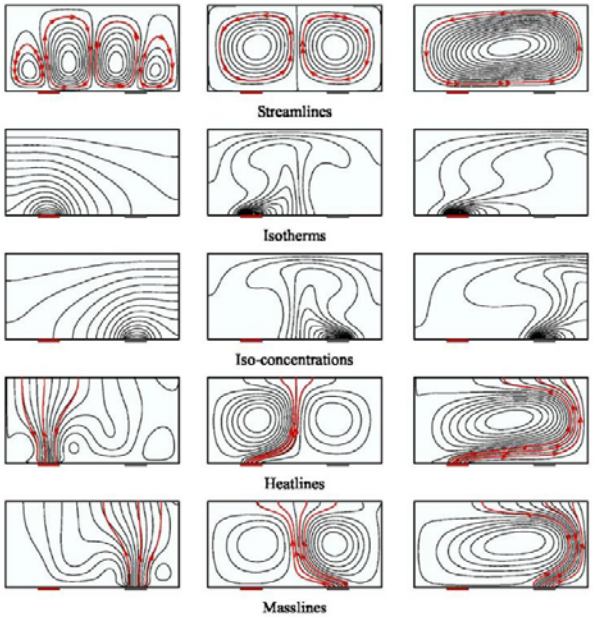

Fig. 3. Contour lines of stream function, temperature, concentration, heat function and mass function for N=1 and Ra_t=2×10^4. (a) Nu= 0.919, Sh= 0.907; (b) Nu= 2.119, Sh= 1.953; (c) Nu= 2.261, Sh= 1.921

3.1 Physical configuration and model

As shown in Fig. 4, three-dimensional ventilated room was modeled with a rectangular parallelepiped. Due to the Coanda effect, this design should allow to the issuing confined wall jet to entrain the air in the whole enclosure. Attention is, the left inlet velocity U_L, width of the enclosure W/H, distance between the center of supplying ports and the bottom wall C/H, and Reynolds number Re on the ventilated air flow should be focused on, due to space constraints, this section payed more attention to supplying jet ports.

3.2 Results and discussion

The average horizontal blowing velocity AU, numerical notation of jet interface shift, is depicted in Fig. 5(a) for $Re = 2 \times 10^5$, $U_L = 1.0$ and $0.05 \leq C/H \leq 0.95$. Multiple steady solutions are obtained by employing different initial conditions, including steady solutions of $U_L = 0.0$, $U_L = 2.0$ and rest state. Generally, the multiple steady solutions occur at $0.15 < C/H < 0.70$, with the AU amplitude of non-symmetrical solutions greatly exceeding 0.1. Outside the range of $0.15 < C/H < 0.7$, the development of the wall jet is limited by the effect of both lateral and vertical confinement due, respectively, to the interaction of the mean flow with the lateral enclosure wall and with top wall or floor. This confinement effect reduces the entrainment of the jet with its surroundings and leads to stabilization of the airflow rate and leads the possible flow states into a single convective mode.

The flow rate FR as a function of supplying ports elevation has been illustrated in Fig. 5(b) for different U_L. Flow rates of steady solutions $U_L = 0.5$ and $U_L = 1.5$

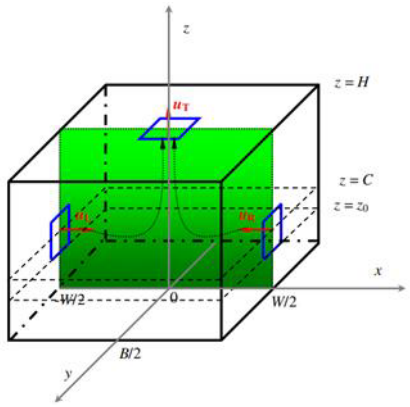

almost parallel each other and present fluctuation of

Fig.4. Schematic view of the full scale ventilated room with three ports of the same dimensions.

double-peak structure with supplying ports *C/H*. *FR* increases with promoting *C/H* and firstly peaks around at *C/H* = 0.2 and then decays to *C/H* = 0.35 where the adverse pressure gradient adjacent to the exhaust port would comparably affect the horizontal blowing flow. Further increasing *C/H* continuously, *FR* again increases abruptly and the maximum flow rate occurs around at *C/H* = 0.7. Subsequently, *FR* decays with the promotion of supplying ports. For the situations of equal-intensity supplying jets (U_L = 1.0), that of symmetrical solutions represented by the delta symbol (using rest state as initial conditions) firstly increases with *C/H*, and almost flats at 0.2 < *C/H* < 0.8. Similar trends can be found for the flow rates of non-symmetrical solutions, respectively, represented by the diamond symbol (using initial conditions of U_L = 2.0) and the gradient symbol (using initial conditions of U_L = 0.0).

4 Mixed convention

The dispersion of airborne pollutant species (such as CO_2) or moisture always accompanies the air flow and thermal transport in built environment [6,7], particularly in industrial space. Based on the traditional mixed convection ventilation, this work further explores the multiply steady solution of air flow, thermal transport and species transport.

4.1 Physical configuration and model

Fig. 6 presents the physical model and the coordinate system, which simplified (*W/H* = 2) the geometry. The heat and pollutant source of length S_{sou}/H = 0.4 was positioned centrally on the floor, whereas the left and right exhaust sides of the same size S_{out}/H = 0.4 and the top middle ceiling inlet of S_{in}/H = 0.4 were attached to this industrial hall. Non-unique steady-state solutions induced by Richardson number was investigated in this section.

4.2 Results and discussion

The effect of the Grashof number on the average Nusselt and Sherwood numbers is depicted in Fig. 7 The results for the configuration (starting at a low *Gr*) indicated that

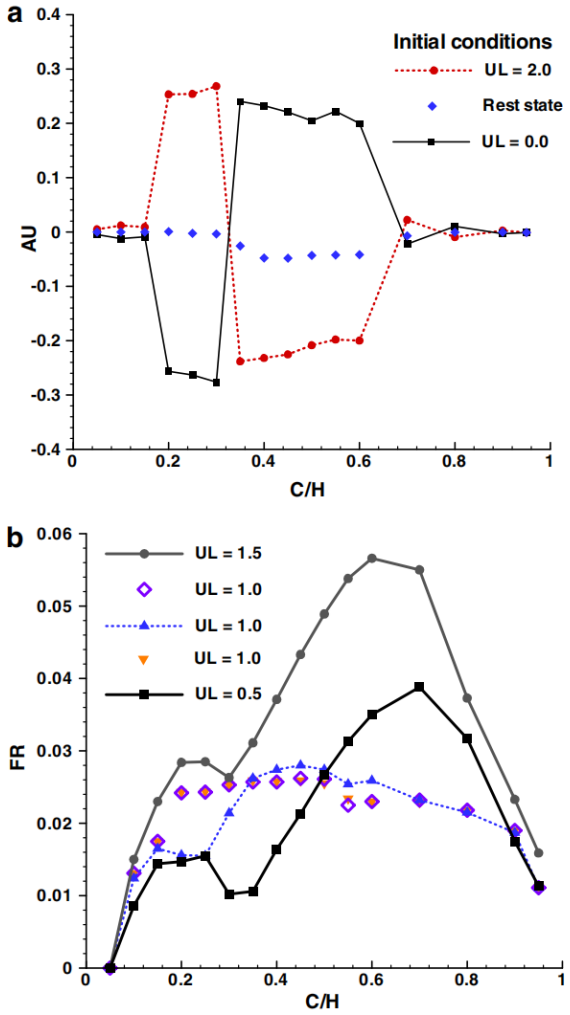

Fig. 5. Average blowing velocity *AU* and flow rate *FR* as functions of supplying ports elevation *C/H* with parameter U_L, and $Re = 2 \times 10^5$. (a) *AU* as a function of *C/H* for U_L = 1.0; (b) *FR* as a function of *C/H*.

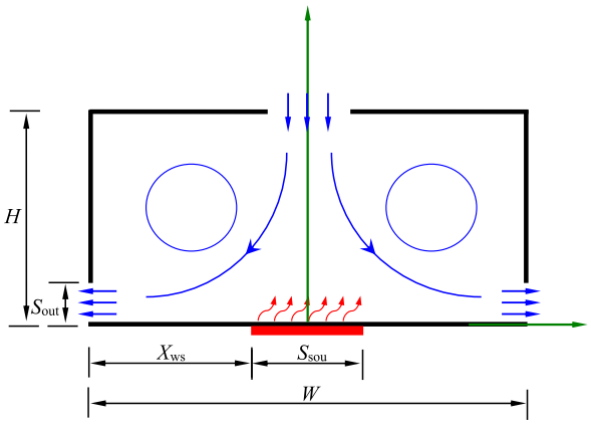

Fig. 6. Geometric illustrations of an industrial ventilation hall and its coordinate system.

the average Nusselt and Sherwood numbers were relatively higher than those starting at a high *Gr*. The average Nusselt and Sherwood numbers increased slightly with increasing Grashof number. On the other hand, for the case of *Gr* decreasing from 10^{13} to 10^7, the *Nu* and *Sh* increased significantly as the magnitude of the forced convection was increased. The evolution of the flow structure during the transition is also depicted in Fig. 7 for different Grashof numbers.

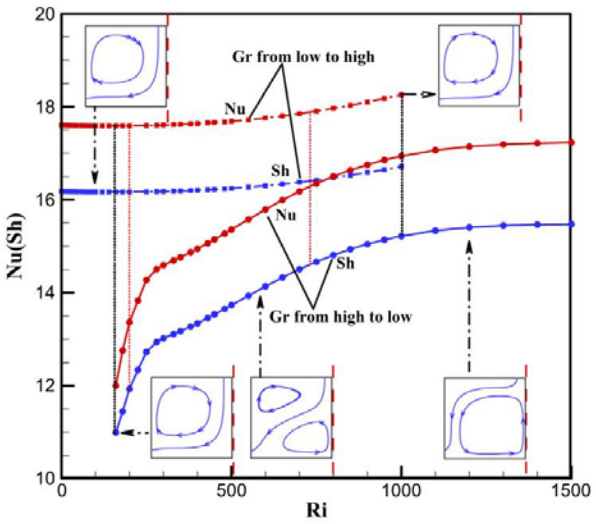

Fig. 7. The effect of the Grashof number on the Nusselt and Sherwood numbers for Re = 10^5.

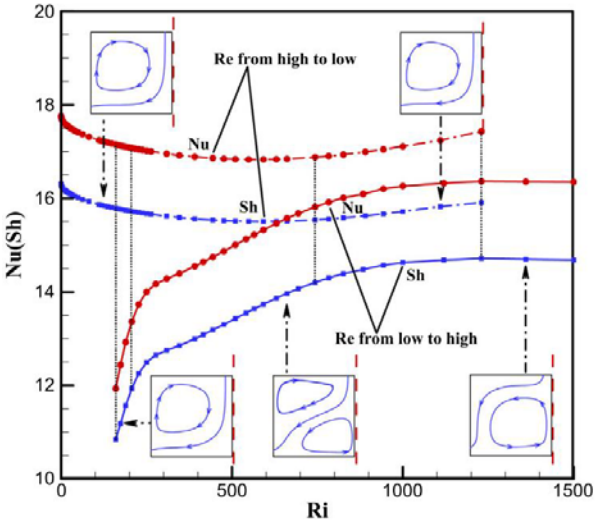

Fig. 8. The effect of the Reynolds number on the Nusselt and Sherwood numbers for Gr = 10^{11}.

The effect of the Reynolds number *Re* on the average Nusselt and Sherwood numbers is illustrated in Fig. 8 for $Gr = 10^{11}$. In Fig. 8, two different possible solutions were found for $150 < Ri < 1000$. Under different initial conditions, the results proved that both forced convection-dominated and thermally dominated flows were possible. The heat and mass transfer by forced convection ($Re = 10^6$ and $Ri = 10^{-1}$ as the initial condition) was obviously enhanced compared with those by natural convection ($Re = 10^4$ and $Ri = 10^3$ as the initial condition). The flow patterns with different vortex structures corresponding to *Nu* and *Sh* are shown in Fig. 8, the evolution of which was identical to that shown in Fig. 7. As expected, in the range of $900 < Ri < 1500$, a thermally induced counter clockwise flow pattern was possible. Furthermore, for $250 < Ri \leq 900$, the wide Reynolds number range mentioned above allowed for a multi-vortex flow. For $150 < Ri \leq 250$ the numerical solutions were found to evolve to the forced convection dominated clockwise circulation.

5 Conclusion

As many of the engineering applications, especially building ventilation, involved diverse convention modes. Multiplicity of linearly stable steady states exists for supercritical natural convection, forced convention and mixed convention in single room building. The existence of a multiplicity of steady-state solutions for the present numerical problem has been demonstrated numerically through the use of appropriate initial perturbations. Single and multiple cell convections take place, depending on the buoyancy ratio, thermal Rayleigh number, Richardson number, jet ports and strip pitch. This work also enables designers to develop ventilation control strategies by avoiding or taking advantages of the multiple flow solutions in building ventilation design. It should be noted that the scope of this study was limited by numerical simulation. Furthermore, future work will be conducted consisting of computational simulation, theoretical analysis and experimental investigation of real space environment multiple steady states.

Authors would gratefully acknowledge the financial supports of Wuhan Application Foundation and Cutting-edge Research Plan (Grant No. 2020010601012206, Wuhan City), Provincial Key R&D Program of Hunan (Grant No. 2022SK2084), Youth Science and Technology Innovation Leader of Hunan Province (Grant No. 2020RC4032), and Natural Science Foundation of China (NSFC Grant No. 51778504, Grant No. U1867221).

References

1. Y.G. Li, P.C. Xu, H. Qian, J.Y. Wu, Flow bifurcation due to opposing buoyancy in two vertically connected open cavities, Int. J. Heat Mass Transf. 49 (2006) 3298–3312.
2. F.Y. Zhao, D. Liu, G.F. Tang, Multiple steady fluid flows in a slot-ventilated enclosure, Int. J. Heat Fluid Flow 29 (2008) 1295–1308.
3. P. Heiselberg, Y.G. Li, A. Andersen, M. Bjerre, Z. Chen, Experimental and CFD evidence of multiple solutions in a naturally ventilated building, Indoor Air. 14 (2004) 43-54.
4. D.D. Zhang, Y. Cai, D. Liu, Y.F. Zhao, Y.G. Li, Dual steady flow solutions of heat and pollutant removal from a slot ventilated welding enclosure containing a bottom heating source, Int. J. Heat Mass Tran. 132 (2019) 11-24.
5. F.Y. Zhao, D. Liu, G.F. Tang, Multiple steady flows in confined gaseous double diffusion with discrete thermosolutal sources, Phys. Fluids. 19 (2007) 107103.
6. J. Xaman, A. Ortiz, G. Alvarez, Y. Chavez, Effect of a contaminant source (CO2) on the air quality in a ventilated room, Energy 36 (2011) 3302–3318
7. D. Liu, F.Y. Zhao, H.Q. Wang, History recovery and source identification of multiple gaseous contaminants releasing with thermal effects in an indoor environment, Int. J. Heat Mass Transf. 55 (2012) 422–435.